Journal of Applied Polymer Science

Preparation and characterization of innovative cellulose diacetate/epoxy resin blends modified by isophorone diamine

Ming Ye, Nianqing Zhu, Zhongbin Ni, Weifu Dong, Mingqing Chen

Key Laboratory of Food Colloids and Biotechnology (Ministry of Education), School of Chemical and Material Engineering, Jiangnan University, 1800 Lihu Road, Wuxi 214122, China

Ming Ye and Nianqing Zhu contributed equally to this article.

Correspondence to: M. Chen (E-mail: mq-chen@jiangnan.edu.cn)

ABSTRACT: Cellulose diacetate (CA)/epoxy resin (EP) blends with excellent mechanical performance were prepared with simple blending followed by curing with isophorone diamine (IPDA). The reaction between the amino groups of IPDA and epoxide groups of EP was confirmed by Fourier transform infrared spectroscopy. Scanning electron microscopy revealed that the cured EP particles gradually became larger and closer to each other to form semi-interpenetrating polymer networks in the CA matrix; this contributed to the improved mechanical properties of the CA/EP blends. Dynamic rheological experiments indicated that the CA/EP blends with semi-interpenetrating polymer networks retained processability. After the introduction of a low content (5–10 phr) of IPDA, the mechanical properties of the CA/EP blends were significantly enhanced. With the addition of 20–30-phr IPDA, the CA/EP blend exhibited a tensile strength of 77 MPa, a flex strength of 65 MPa, a flex modulus of 2.6 GPa, and a hardness of 94 HD; these values were much higher than those of the pristine CA/EP binary blend. © 2016 Wiley Periodicals, Inc. J. Appl. Polym. Sci. **2016**, *133*, 44151.

KEYWORDS: biomaterials; blends; crosslinking; structure–property relations; thermoplastics

Received 7 May 2016; accepted 4 July 2016

DOI: 10.1002/app.44151

INTRODUCTION

There is growing interest in the environmental protection of the earth because the environmental situation of the earth is worse than that in old times.[1] Although traditional engineered thermoplastics with good mechanical properties, such as polyamide, polycarbonate, polyformaldehyde, poly(butylene terephthalate), and poly(phenylene oxide),[2–6] can be used as a structural material to bear mechanical stress, these traditional materials are responsible for worsening environmental conditions because of their absence of degradable properties. If all traditional thermoplastics were made from biodegradable polymers, these environmental problems would be solved. However, the comprehensive performance of some biodegradable polymers, such as polylactide, poly(butylene succinate), and poly(ε-caprolactone), are not stable.[7–10] Polylactide is a biodegradable aliphatic polyester with excellent properties for various applications. However, the disadvantages of its brittleness and low heat distortion temperature limit its widespread applications.[11]

Cellulose diacetate (CA), the most widely used cellulose derivatives at present, is a kind of environmentally friendly material with a good biodegradable nature and mechanical properties.[12,13] Usually, CA materials are processed by a solution method, especially in the field of spinning. Yu *et al.*[14] prepared CA fibers spun from a CA spinning dope, which contained acetone solvent. A method of dry-spun CA fibers with celluose nanocrystals (CNC) as reinforcements was presented by Chen *et al.*[15] CA–CNC solutions were first mixed together in a round-bottom flask with agitation. Because of the high porosity and uniform pore diameter of CA, some researchers have applied it in the field of membranes. A novel aliphatic hyperbranched polyester modified CA membrane exhibited a low flux, high hydraulic resistance, and good thermal and mechanical properties.[16]

The intermolecular force of CA is large because of the large number of hydroxyl groups, acetyl groups, and other polar groups contained in the CA molecular chain. Moreover, its melting temperature is very close to the thermal decomposition temperature. Thus, CA cannot be processed with conventional techniques, such as extrusion and injection molding. To process CA, extra additives should be added. In the melting process, conventional plasticizers, such as glycerin triacetate, tributyl citrate, and dioctyl phthalate, are usually used to improve the CA molecular chain's mobility and to reduce the melt-processing temperature.[17,18] The melt blending of CA with poly(butylene succinate), poly(methyl methacrylate), and nanoclay for biodegradable plastic applications has been reported in recent

literature. However, because of the short molecular chain, these plasticizers slowly escape from plastic products into air, soil, water, and food. Moreover, the migration of plasticizers lead to a reduction in the mechanical strength.[19] Accordingly, high molecular plasticizers need to be used. Liquid epoxy resin (EP) contains a large number of epoxy groups and hydroxyls, which have good compatibility with CA, which contains a lot of ester bonds.[20] Moreover, the molecular chains of liquid EP are longer than those of conventional plasticizers.[21–24]

In this study, we attempted to produce a simple route for preparing biobased CA/EP blends. EP was used as the plasticizer. To enhance the mechanical performance, an appropriate amount of the curing agent isophorone diamine (IPDA) was added. During the first stage, CA, EP, and IPDA were fully blended with a torque rheometer. An extra amount of acetone was added to swell the CA molecular chains in the compounding process. Next, the interspersed EP molecular chains in the CA matrix were cured by IPDA at a higher temperature. The structure and properties of the CA/EP blends were systematically investigated by Fourier transform infrared (FTIR)spectroscopy, scanning electron microscopy (SEM), gel content analysis, rheological testing, and mechanical testing. SEM revealed that partially cured EP formed semi-interpenetrating polymer networks in the matrix of CA. This study not only provided a fundamental investigation of CA/EP-based semi-interpenetrating polymer networks but also broadened the application ranges of both CA and EP.

EXPERIMENTAL

Materials

CA (chemical product for plastic use), with a degree of substitution of 2.25 and a relative density of 1.28–1.32 g/cm^3 (1 g/cm^3 for water), was purchased from Sichuan Push Acetati Co., Ltd. (Sichuan, China). The purity of CA was more than 95%. Bisphenol A EP, with a viscosity of 2500 mPa s at 40 °C (E51), was supplied by Wuxi A Erzi Chemical Co., Ltd. (Wuxi, China). The epoxy value of the EP was 0.48–0.54 equiv/100 g. IPDA (purity ≥ 99.7%) was supplied by BASF SE (Germany). Acetone (purity ≥ 99.5%) was purchased from Sinopharm Chemical Reagent Co., Ltd. (China). Diacetone alcohol (DAA; purity ≥ 98.5%) was supplied by Yonghua Chemical Technology Co., Ltd. (China). All of the chemicals were used as received.

Sample Preparation

Before blending, CA and EP were dried overnight in a vacuum oven at 80 and 60 °C, respectively. To the fully mixed CA and EP, mixed solvent was added with acetone and DAA with a ratio of 95/5 (w/w). Because acetone was a good solvent for CA and DAA is a good solvent for EP, the mixed solvent was fully stirred with a stirring rod. Because the IPDA content is very crucial to the structure and properties of the CA/EP blends, different amounts of IPDA (0–30 phr on the basis of EP) were investigated, whereas the weight ratio of CA/EP was fixed at 70/30 (w/w). Different amounts of IPDA were added to a pre-equipped mixed solvent and stirred until the mixture was smooth. The CA/EP was agitated with the mixed solvent (25 phr on the basis of CA/EP) containing IPDA. Next, the premix

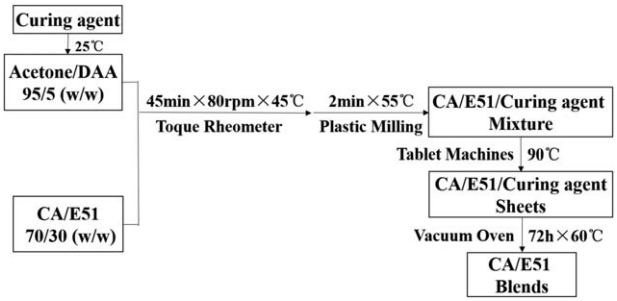

Scheme 1. Preparation routes of the CA/EP blends.

was added to a torque rheometer (Haake Polylab-OS, Thermo Fisher Scientific, Inc., Germany) for 45 min at a rotor speed of 80 rpm to form a homogeneous CA/EP/IPDA compound at 45 °C. The CA/EP/IPDA compounds were then mixed in a plastic mill (KY-3203-C, Kaiyan Mechanical Equipment Co., Ltd., Taiwan, China) for 2 min at 55 °C to volatile solvent and to increase the molecular compactness. All of the samples were compression-molded into sheets (0.5 mm and 4 mm in thickness) at 90 °C for 5 min. The compression-molded samples were put in a vacuum oven at 60 °C for 72 h and were finally used for characterizations. The aforementioned preparation routes are summarized in Scheme 1.

Characterization

Gel Fraction Measurement. The compression-molded samples with a predetermined weight (ω_1) were dissolved in acetone for 1 week and then stirred and refluxed at 60 °C for 2 days to thoroughly dissolve all of the uncured parts. The suspensions were then centrifuged twice at 8000 rpm to enable the cured parts to gather at the bottom of the centrifuge tube. The upper-layer clear solution was poured out. The cured specimens were added with excess acetone and DAA for certain washing times and were then dried in a vacuum oven at 60 °C until the mass change was less than 0.1 mg. The dried residuals, defined as the *gel* in this study, were then weighed to an accuracy of 0.1 mg (ω_2). The gel fractions were calculated by the following equation:

$$\text{Gel fraction} = (\omega_2/\omega_1) \times 100\% \quad (1)$$

Attenuated Total Reflection (ATR)–FTIR. ATR–FTIR spectroscopy (Nicolet 6700, Thermo Fisher Technology Co., Ltd.) analysis of the EP gel, EP, IPDA, and CA was carried out in the range 4000–400 cm^{-1}. The test resolution was 2 cm^{-1}, and the scanning time was 16.

SEM. SEM (S-4800, Hitachi Metals Group, Japan) was used to observe the morphology of the fractured surfaces of specimens and surfaces etched by acetone. Both tensile-fractured surfaces of compression-molded specimens were observed with an accelerating voltage of 4 kV and 10 kV, whereas the etched cross section was observed with an accelerating voltage of 4 kV. Before SEM characterization, the fractured surface was sputtered with a layer of gold.

Rheological Behavior. Dynamic rheological experiments were carried out on a DHR-2 rheometer (TA Instruments) in a plate–plate configuration (25 mm in diameter and 1 mm in gap)

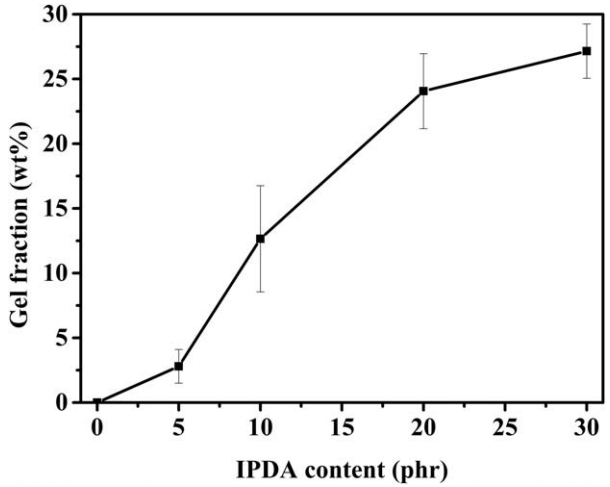

Figure 1. Gel fractions for the pristine CA/EP and CA/EP blends with different contents of IPDA.

at 200 °C. The samples were tested in frequency-sweep mode (from 100 to 0.01 Hz) with an optimal strain of 1%. The optimal strain was predetermined from a strain–sweep experiment to ensure that the measurements were performed in the linear viscoelastic strain range.

Mechanical Properties. The tensile properties of the CA/EP blends were measured with a universal tensile tester (Instron 5967) according to GB/T528-2009 at a tensile speed of 50 mm/min. The dimension of the parallel section of the tensile bar was $25 \times 4 \times 0.5\ mm^3$. The flexural property were measured with a universal tensile tester (Instron 5967) according to GB/T 9341-2008 at a flexural speed of 2 mm/min. Five specimens of each sample were tested, and the averaged results are presented. The hardness was measured with a Shore D hardness tester (LX-D, Qianzhou Measuring Instrument, Wuxi, China) according to GB/T 531.1-2008.

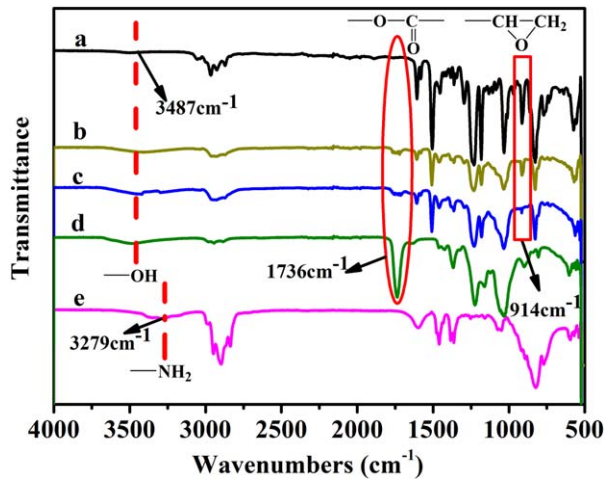

Figure 2. FTIR spectra of the (a) neat EP, (b) 10-phr EP gel, (c) 30-phr EP gel, (d) CA, and (e) IPDA. [Color figure can be viewed in the online issue, which is available at wileyonlinelibrary.com.]

RESULTS AND DISCUSSION

Gel Content Analysis of the CA/EP Blends

A clear solution was observed for the pristine CA/EP blends in acetone and DAA; this indicated a lack of solidification. This behavior changed with the addition of IPDA. A crosslink structure (gel) was generated after the addition of the curing agent IPDA to the CA/EP blends. The structure and composition of the gel were very important to the phase morphology and mechanical properties of the CA/EP blends.[25] The gel content of the CA/EP blends as a function of the IPDA content was measured, as shown in Figure 1. The gel fractions of the CA/EP blends increased to 27.15 wt % when the IPDA content increased to 30 phr. These results indicate that the crosslink density of the gel increased with increasing IPDA content.

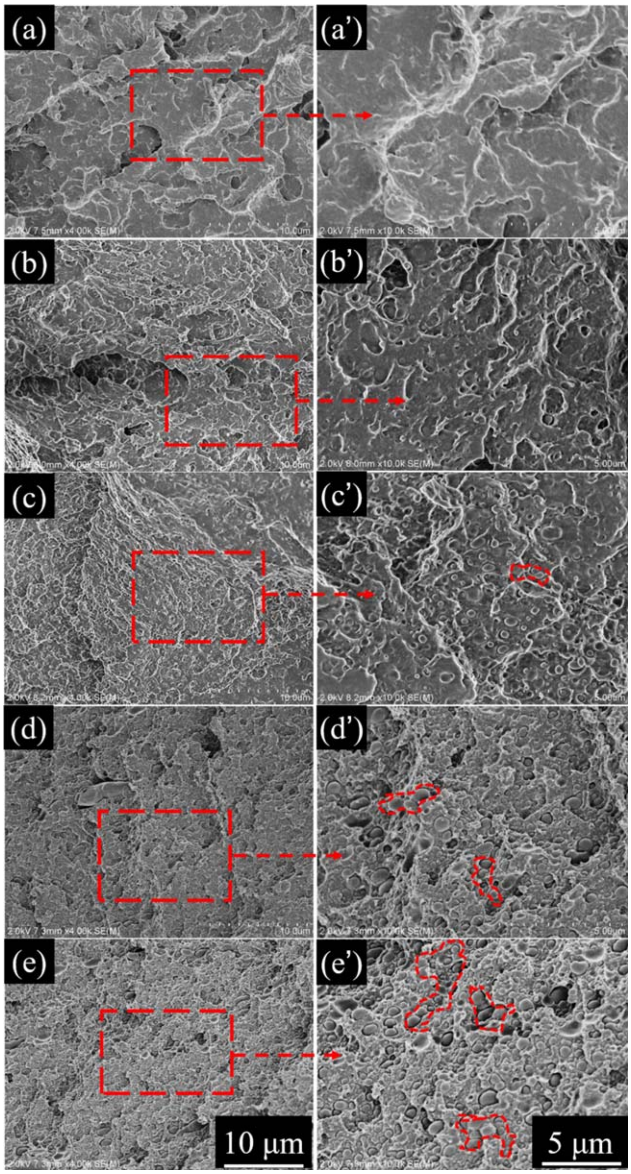

Figure 3. SEM images of the tensile-fractured surfaces of CA/EP blends with various amounts of IPDA: (a,a′) 0, (b,b′) 5, (c,c′) 10, (d,d′) 20, and (e,e′) 30 phr. [Color figure can be viewed in the online issue, which is available at wileyonlinelibrary.com.]

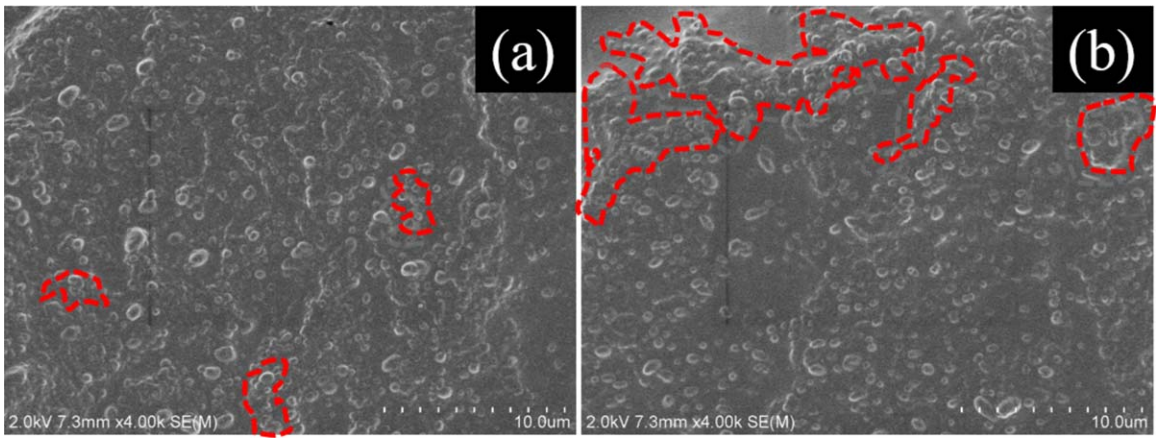

Figure 4. SEM images of the tensile-fractured surfaces of CA/EP blends etched by acetone with various amounts of IPDA: (a) 20 and (b) 30 phr. [Color figure can be viewed in the online issue, which is available at wileyonlinelibrary.com.]

However, the crosslink density of the gel was slightly lower than the theoretical value. In the static solidification process, the reactive groups of epoxide and amine only reacted until they met together. In other words, some of these reactive groups existed in free form because of the fact that the molecular chains were not moving and the distance between these groups was far away.

ATR–FTIR Analysis of the CA/EP Blends

The chemical structures of the neat EP, 10-phr EP gel, 30-phr EP gel, CA, and IPDA were determined by FTIR spectroscopy. The typical FTIR spectra of the neat EP, 10-phr EP gel, 30-phr EP gel, CA, and IPDA are presented in Figure 2. For neat EP [Figure 2(a)], the characteristic absorption bond at 3487 cm^{-1} corresponded to O—H stretching vibration of hydroxyl groups; 2965 cm^{-1} and 2927 cm^{-1}, corresponded to C—H stretching vibrations; 1606 cm^{-1}, 1581 cm^{-1}, 1507 cm^{-1} and 1384 cm^{-1} corresponded to benzene stretching vibrations; 1461 cm^{-1} corresponded to C—O stretching vibration; 914 cm^{-1} corresponded to the epoxy-terminated groups.[26–28] When blending with IPDA, the peak intensity at 914 cm^{-1} became smaller, and the absorption strength decreased with increasing IPDA content [Figure 2(b,c)]. This change confirmed the reaction between epoxy groups and amino groups. The wide absorption band at about 3279 cm^{-1} was attributed to N—H stretching vibrations in IPDA [Figure 2(e)],[29] but it was absent in the EP gel [Figure 2(b,c)]. This indicated that epoxy groups in the blends were excessive.

For CA [Figure 2(d)], the peak at about 1736 cm^{-1} corresponded to C=O stretching vibrations, which are commonly influenced by the conjugation effect of benzene and the inductive effect in virtue of alkyl groups.[30] There was a small peak at about 1736 cm^{-1} for the EP gel [Figure 2(b,c)], but this peak was absent for neat EP [Figure 2(a)]. This indicated the existence of CA chains. In addition, the hydroxyl groups of CA chains might have reacted with epoxide under certain conditions. Therefore, the gel of the CA/EP blends might have consisted of the hybrid reaction products derived from EP, CA, and IPDA.

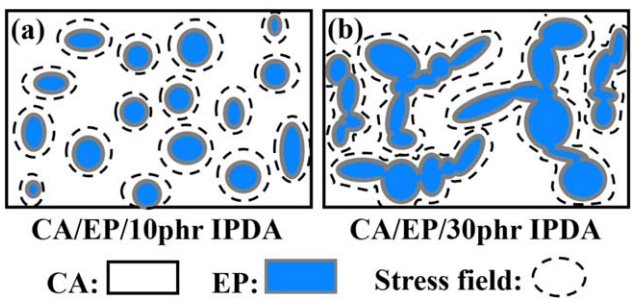

Figure 5. Schematic representation of the deformation mechanisms of CA/EP blends with and without IPDA: (a) CA/EP/10-phr IPDA and (b) CA/EP/30-phr IPDA. [Color figure can be viewed in the online issue, which is available at wileyonlinelibrary.com.]

Morphology of the CA/EP Blends

The phase morphologies of the pristine CA/EP binary blend and CA/EP blends modified by IPDA were characterized by SEM. Figure 3 shows the SEM images of the tensile-fractured surfaces of the pristine CA/EP binary blend and CA/EP blends modified by IPDA. The pristine CA/EP blends showed good compatibility [Figure 3(a,a′)]. However, the CA/EP blends modified by IPDA exhibited an obvious phase-separation structure with the cured EP phase dispersed in the CA matrix with irregular shapes [Figure 3(b–e,b′–e′)]; this implied incompatibility between the two phases. When 5-phr IPDA was added, obvious phase separation was observed [Figure 3(b,b′)]; the compatibility seemed to be degraded, and some spongelike aggregates with irregular shapes were captured. When the content of IPDA was increased further, in some domains, the gaps between the surfaces of the cured EP and CA phases were easily observed [Figure 3(c,c′)]; this reflected poor interfacial adhesion between the cured EP and CA because of interfacial tension between the two phases.

The CA/EP blends modified by IPDA displayed a good sea-island structure with discretely cured EP islands embedded in a CA matrix sea [Figure 3(b,b′)]. Meanwhile, when 20- or 30-phr IPDA was added, sea-island structure gradually turned into EP clusters, and the discretely cured EP islands gradually became larger and closer to each other. In other words, some bulklike and rodlike aggregates of the cured EP evidently tended to

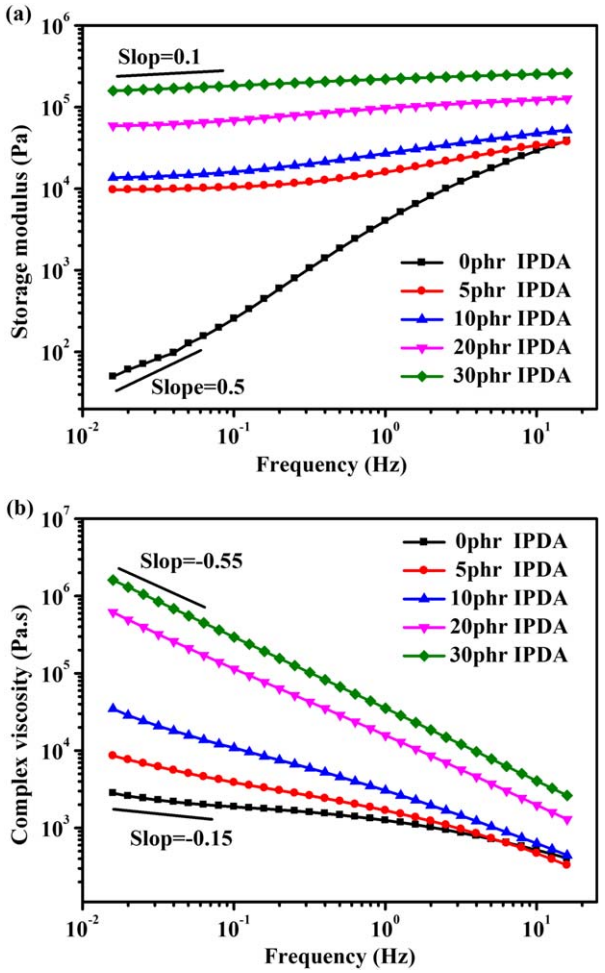

Figure 6. (a) G' and (b) η^* values of the CA/EP blends as a function of the frequency and IPDA content. [Color figure can be viewed in the online issue, which is available at wileyonlinelibrary.com.]

connect with each other to form semi-interpenetrating polymer networks[31,32] [as highlighted by the red circles in Figure 3(c′–e′)], although obviously incompatible were observed.

To further verify this observation, an etched cross section was used for SEM inspection. As shown in Figure 4, the cured EP formed semi-interpenetrating polymer networks in the CA matrix. The structure of the CA/EP blends with two different phases is shown in Figure 5.[33] For the blend with a sea-island structure, the stress fields around the cured EP particles could not interact with each other [Figure 5(a)]. In this condition, EP had a toughening effect on the CA matrix. However, the toughness of the CA/EP blend decreased when 10-phr IPDA was added. This was attributed to the poor compatibility between CA and EP (as highlighted by the gray circles in Figure 5). In addition, for the blends with a semi-interpenetrating polymer network structure, the stress fields around the EP particles localized in the networklike band could easily overlap, sharing some of the force generated by the outside world; therefore, this resulted in an excellent strengthening effect. That is, the semi-interpenetrating polymer networks could act as a path for the propagation of the stress needed for effective energy dissipation. Furthermore, the EP networklike steel, which was composed of elongated particles, could take more external force.

Rheological Behavior of the CA/EP Blends

Rheology has been proven to be a powerful technique for investigating the structures of polymers and polymer blends. The storage modulus (G') and the complex viscosity (η^*) of the CA/EP blends as a function of the frequency are shown in Figure 6. G' and η^* of the CA/EP blends were significantly affected by

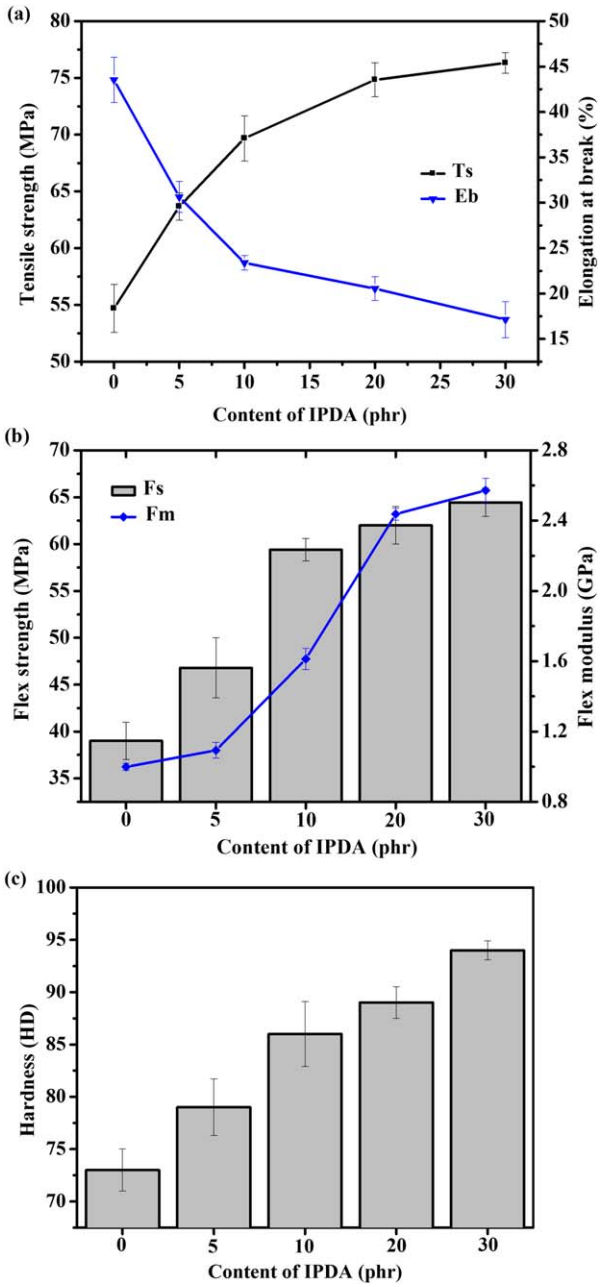

Figure 7. (a) Tensile properties, (b) flexural properties, and (c) hardness of the CA/EP (70/30) blends and CA/EP (70/30) blends modified by IPDA (Eb = elongation at break; Fm = flexural modulus; Fs = flexural strength; Ts = tensile strength). [Color figure can be viewed in the online issue, which is available at wileyonlinelibrary.com.]

the formed semi-interpenetrating polymer networks. A sharp increase in both G' and η^* with increasing IPDA content at a frequency (ω) of less than 1 Hz; this indicated that the melt viscoelasticity of the CA/EP blends increased. When the frequency approached 0.01 Hz, the slope of log G' versus log ω decreased from 0.5 to 0.1 with increasing IPDA content up to 30 phr [Figure 6(a)]. Meanwhile, the slope of log η^* versus log ω reduced from -0.15 to -0.55 [Figure 6(b)]. Apparently, the CA/EP blends showed a pseudo-solidlike behavior in the low-frequency zone because of the presence of semi-interpenetrating polymer networks. These results were in accordance with the gel analysis. It should be noted that all of the samples exhibited similar viscosities in the high-frequency zone; this indicated that the CA/EP retained its processability after crosslinking.

Mechanical Properties of the CA/EP Blends

To evaluate the influence of semi-interpenetrating polymer networks induced by IPDA on the mechanical properties of the CA/EP blends, the flexural properties and tensile properties were measured. Figure 7(a) shows the tensile properties of the CA/EP blends modified by IPDA. Interestingly, the introduction of IPDA resulted in a significant improvement in the tensile strength of the CA/EP blend. The tensile strength was dramatically enhanced from 54.70 to 76.32 MPa with the IPDA content increased from 0 to 30 phr; however, the elongation at break decreased from 43.53 to 17.13%. More importantly, the strengthen efficiency was found to be greatly dependent on the phase structure of the CA/EP blends. Compared with the cocontinuous structure, semi-interpenetrating polymer networks endowed the blends with a better tensile strength. Moreover, it should be noted that an excellent strengthening effect was achieved without sacrificing the elongation at break at a 5 phr addition of IPDA [Figure 7(a)]. In this case, only a small amount of EP was cured and part of the EP acted as a plasticizer.

The flexural data [Figure 7(b)] showed similar results for all the CA/EP blends with respect to their tensile properties. The flexural strength maintained an increasing trend, whereas the flexural modulus increased with increasing IPDA content. The hardness of the blends is presented in Figure 7(c). The changing trend of the hardness was consistent with that of the modulus [Figure 7(b,c)]. This might have been due to the formation of semi-interpenetrating polymer networks in the CA/EP blends. The cured EP made the chains connect more closely inside the CA/EP blends; this resulted in an enhanced hardness.

CONCLUSIONS

In this study, a series of CA/EP blends with excellent mechanical performances was prepared. The addition of the curing agent IPDA into the blends resulted in the formation of a special semi-interpenetrating polymer network structure. The induced semi-interpenetrating polymer networks structure imparted the CA/EP blends with improved tensile strength, hardness, flex strength, and modulus. This study provided a simple but effective strategy for preparing CA-based materials with a good stiffness–processing property balance.

ACKNOWLEDGMENTS

This work was supported by the National Natural Science Foundation of China (contract grant number 21571084)

REFERENCES

1. Ikezaki, T.; Matsuoka, R.; Hatanaka, K.; Yoshie, N. *J. Polym. Sci. Part A: Polym. Chem.* **2013**, *52*, 216.
2. Chow, W. S.; Mohd, I. Z. A. *Express Polym. Lett.* **2015**, *9*, 211.
3. Sophie, M. G.; Laetitia, M. *J. Appl. Polym. Sci.* **2014**, *131*, DOI: 10.1002/app.40081.
4. Baldi, F.; Bongiorno, A.; Fassi, I.; Franceschini, A.; Pagano, C.; Riccò, T.; Surace, R.; Tescione, F. *Polym. Eng. Sci.* **2014**, *54*, 512.
5. Chiu, S. J.; Wu, Y. S. *J. Anal. Appl. Pyrol.* **2009**, *86*, 22.
6. Wu, Y.; Zhang, H.; Shentu, B.; Weng, Z. *Ind. Eng. Chem. Res.* **2015**, *54*, 5870.
7. Racha, A.; Khalid, L.; Abderrahim, M. *Eur. Polym. J.* **2014**, *58*, 90.
8. Xu, J.; Guo, B. H. *Biotechnol. J.* **2010**, *5*, 1149.
9. Sophie, R.; Lan, T.; Françoise, B.; Bruno, V. *J. Appl. Polym. Sci.* **2014**, *131*, DOI: 10.1002/app.40364.
10. Erde, C.; Seyda, B.; Emre, K.; Ayşe, C. Ç.; Gamze, T. K. *Polym. Plast. Technol.* **2014**, *53*, 1178.
11. Mary, K. M.; Douglas, E. H. *Polym. Eng. Sci.* **2015**, *55*, 1652.
12. Charles, M. B.; Robert, M. G.; Ronald, J. K. *J. Appl. Polym. Sci.* **1993**, *47*, 1709.
13. Kevin, J. E.; Charles, M. B.; John, S. D.; Paul, A. R.; Brian, D. S.; Michael, C. S.; Debra, T. *Prog. Polym. Sci.* **2001**, *26*, 1605.
14. Yu, Q.; Xu, X.; Zhang, L.; Cao, J.; Deng, C.; Wang, Q.; Fan, X. *Fibers Polym.* **2015**, *16*, 105.
15. Chen, S.; Greg, S.; Pipes, B. R.; Jeffrey, Y.; Robert, J. M. *Biomacromolecules* **2014**, *15*, 3827.
16. Mahdavi, H.; Taieb, S. *J. Membr. Sci.* **2015**, *473*, 256.
17. Jackson, E. A.; Aji, P. M.; Kristiina, O. *J. Appl. Polym. Sci.* **2009**, *114*, 2723.
18. Mohanty, A. K.; Wibowo, A.; Misra, M.; Drzal, L. T. *Polym. Eng. Sci.* **2003**, *43*, 1151.
19. Farzaneh, A.; Naser, M. *Carbohydr. Polym.* **2015**, *130*, 316.
20. Alamri, H.; Low, I. M. *Polym. Compos.* **2012**, *33*, 589.
21. Wang, W.; Diao, E.; Zhang, H.; Dai, Y.; Hou, H.; Dong, H. *J. Appl. Polym. Sci.* **2015**, *132*, DOI: 10.1002/app.42544.
22. Chaowei, P.; Robert, A. S.; Fugen, D. *Compos. A* **2015**, *70*, 52.
23. Liu, H.; Xiao, C.; Hu, X. *Desalination Water Treat.* **2013**, *51*, 3786.
24. Szarka, G.; Iván, B. *J. Macromol. Sci. A.* **2013**, *50*, 208.
25. Ma, P.; Xu, P.; Liu, W.; Zhai, Y.; Dong, W.; Zhang, Y.; Chen, M. *RSC Adv.* **2015**, *5*, 15962.
26. Deng, J.; Liu, X.; Li, C.; Jiang, Y.; Zhu, J. *RSC Adv.* **2015**, *5*, 15930.

27. Wang, Y.; Wang, Z.; Ma, P.; Bai, H.; Dong, W.; Xie, Y.; Chen, M. *RSC Adv.* **2015**, *5*, 72691.
28. Dai, X.; Xiong, Z.; Ma, X.; Li, C.; Wang, J.; Na, H.; Zhu, J. *Ind. Eng. Chem. Res.* **2015**, *54*, 3806.
29. Achilias, D. S.; Karabela, M. M.; Varkopoulou, E. A.; Sideridou, I. D. *J. Macromol. Sci. Chem.* **2012**, *49*, 630.
30. Manjunath, L.; Sailaja, R. R. N. *Cellulose* **2014**, *21*, 1793.
31. Xu, X.; Hossein, T. *Polym. Eng. Sci.* **2000**, *40*, 2027.
32. Charles, U. P. J.; Xu, X.; Lichang, W.; Hossein, T. *Polym. Eng. Sci.* **2000**, *40*, 1405.
33. Xiu, H.; Huang, C.; Bai, H.; Jiang, J.; Chen, F.; Deng, H.; Wang, K.; Zhang, Q.; Fu, Q. *Polymer* **2014**, *55*, 1593.